Global transcriptional profiling of the postmortem brain of a patient with G114V genetic Creutzfeldt-Jakob disease

CHAN TIAN[1*], DI LIU[2*], CHEN CHEN[3], YIN XU[1], HAN-SHI GONG[1,4], CAO CHEN[1], QI SHI[1], BAO-YUN ZHANG[1], JUN HAN[1] and XIAO-PING DONG[1]

[1]State Key Laboratory for Infectious Disease Prevention and Control, National Institute for Viral Disease Control and Prevention, Chinese Center for Disease Control and Prevention, Beijing 102206; [2]Network Information Center, Institute of Microbiology, Chinese Academy of Sciences, Beijing 100101; [3]State Key Laboratory for Infectious Disease Prevention and Control, National Institute for Communicable Disease Control and Prevention, Chinese Center for Disease Control and Prevention, Beijing 102206; [4]School of Medicine, Xi'an Jiao Tong University, Xi'an, Shaanxi 710061, P.R. China

Received October 22, 2012; Accepted December 18, 2012

DOI: 10.3892/ijmm.2013.1239

Abstract. Familial or genetic Creutzfeldt-Jakob disease (fCJD or gCJD) is an inherent human prion disease caused by mutation of the prion protein gene (*PRNP*). In the present study, global expression patterns of the parietal cortex from a patient with G114V gCJD were analyzed using the Affymetrix Human Genome U133+ 2.0 chip with a commercial normal human parietal cortex RNA pool as a normal control. In total, 8,774 genes showed differential expression; among them 2,769 genes were upregulated and 6,005 genes were downregulated. The reliability of the results was confirmed using real-time RT-PCR assays. The most differentially expressed genes (DEGs) were involved in transcription regulation, ion transport, transcription, cell adhesion, and signal transduction. The genes associated with gliosis were upregulated and the genes marked for neurons were downregulated, while the transcription of the *PRNP* gene remained unaltered. A total of 169 different pathways exhibited significant changes in the brain of G114V gCJD. The most significantly regulated pathways included Alzheimer's and Parkinson's disease, oxidative phosphorylation, regulation of actin cytoskeleton, MAPK signaling and proteasome, which have previously been linked to prion diseases. In addition, we found some pathways that have rarely been explored in regards to prion diseases that were also significantly altered in G114V gCJD, such as axon guidance, gap junction and purine metabolism. The majority of the genes in the 10 most altered pathways were downregulated. The data of the present study provide useful insights into the pathogenesis of G114V gCJD and potential biomarkers for diagnostic and therapeutic purposes.

Correspondence to: Professor Xiao-Ping Dong, State Key Laboratory for Infectious Disease Prevention and Control, National Institute for Viral Disease Control and Prevention, Chinese Center for Disease Control and Prevention, 155 Chang-Bai Road, Beijing 102206, P.R. China
E-mail: dongxp238@sina.com

*Contributed equally

Key words: Creutzfeldt-Jakob disease, familial Creutzfeldt-Jakob disease, gene chip, expression pattern, microarray

Introduction

Prion diseases, also known as transmissible spongiform encephalopathies (TSEs), are a group of fatal neurodegenerative disorders in humans and animals, including Creutzfeldt-Jakob disease (CJD) in humans, bovine spongiform encephalopathies (BSEs) in cattle, and scrapie in sheep and goats. The conversion of prion protein (PrP), coded by the *PRNP* gene, from its cellular isoform PrP^{C} to its pathogenic isoform PrP^{Sc} through a post-translational process is considered the etiology of these diseases. As a result of the conversion, the portion of β-sheets within PrP is increased (from 3 to 45%) whereas that of α-helices decreases (from 42 to 30%), therefore causing PrP to become detergent insoluble and resistant to denaturant (isoform PrP^{Sc}) (1). The conversion also causes a series of histopathological changes, including the depositions of PrP^{Sc}, spongiform degenerations, neuronal loss and astrogliosis.

According to the pathomechanisms, CJD can be classified into sporadic CJD (sCJD), familial or genetic CJD (fCJD or gCJD) and iatrogenic CJD (iCJD). fCJD accounts for approximately 10-15% of all CJD cases, characterized by the genetic changes of PrP (2). To date, 56 different mutations, including residue substitutions, insertions and deletions, have been reported (3). For instance, proline to leucine mutation at the 102nd position (P102L) causes Gerstmann-Straussler-Scheinker syndrome (GSS) characterized by the impairment of cerebellum (4). Nevertheless, D178N leads to fatal familial insomnia (FFI) (4), mainly harming the thalamus region. The varied clinical manifestations indicate that different mutants may trigger different regulatory pathways.

An efficient approach to uncovering the regulated genes and the signaling pathways caused by PrP^{Sc} is using global transcriptional profiling on prion-infected samples. Studies on various prion strains in mice by Hwang *et al* (5) described a

network of differentially expressed genes (DEGs) on functional pathways and discovered that the gliosis fibril acidic protein gene (Gfap) and a set of complement activation associated genes are highly expressed (5). Xiang *et al* (6) performed their studies using human sCJD brains and described the upregulation of immune and stress-response factors and elements involved in cell death and cell cycle, and the downregulation of genes encoding synaptic proteins (6). However, there is a lack of information on the global transcriptional profiles of gCJD patients, since gCJD and sCJD may utilize different regulatory mechanisms.

In our previous study, we reported a Chinese gCJD patient with a G114V mutation in PrP (7), showing an sCJD-like neuropathological abnormality with large amounts of PrP^{Sc} deposit, spongiform degeneration, astrogliosis and neuron loss in the cortex regions (8). To further investigate the molecular mechanisms and to compare those with sCJD, the full transcriptome pattern of the parietal cortex lobe of this G114V gCJD patient was profiled with microarray analysis (Affymetrix Human Genome U133+ 2.0 Chip) with a commercial normal human parietal cortex RNA pool as control. This investigation revealed numerous DEGs and pathways and our results provide information regarding gCJD that is useful for the development of novel diagnostic and therapeutic approaches.

Materials and methods

Brain sample of the G114V fCJD patient. Brain tissue of the parietal cortex obtained from a patient definitely diagnosed with G114V gCJD was enrolled in this study. The patient was a 47-year-old (at onset) Han-Chinese woman, whose clinical and genetic characteristics have previously been described (7). Neuropathological assays of 10 different brain regions revealed typical sCJD-like abnormality and PrP^{Sc} deposits (8). A commercial normal human parietal cortex total RNA (cat. #636571; Clontech) pooled from four males/females aged 35-89 years was utilized as a control. Usage of the stored human brain samples in this study was approved by the Ethics Committee of the National Institute for Viral Disease Prevention and Control, China CDC. We obtained written informed consent from all participants in our study.

Microarray analysis. Total RNA of the parietal cortex of the patient with G114V gCJD was extracted with an RNeasy Mini kit (cat. #74104; Qiagen), according to the manufacturer's instructions. The quality and quantity of extracted RNAs were verified by 1.2% formaldehyde agarose electrophoresis and ultraviolet spectrophotometry (NanoDrop, ND-1000). The processes of labeling, hybridization and scanning were performed at a platform of CapitalBio Corporation. Briefly, 200 ng of each total RNA preparation was taken for synthesis and amplification of first strand cDNAs, double-stranded cDNAs and biotin-labeled antisense RNAs, using a MessageAmp™ Premier RNA Amplification kit (cat. #AM1792; Ambion) on a PCR apparatus (MJ, PTC-225). After measuring the concentrations of the labeled RNAs by ultraviolet spectrophotometry, 15 μg of each preparation was fragmented and verified using 1.2% formaldehyde denatured agarose electrophoresis.

The biotinylated cRNAs were hybridized to a commercial gene chip, GeneChip® Human Genome U133+ 2.0 (Affymetrix Inc., Santa Clara, CA, USA) containing 47,000 transcripts, at 45˚C for 16 h with constant rotation at a speed of 60 rpm. After washing and staining automatically on an Affymetrix fluidics station 450 with a GeneChip Hybridization, Wash and Stain kit (cat. #900720; Affymetrix), the chips were then scanned on Affymetrix scanners 3000 7G.

After scanning the gene chips, the CEL images were processed using the Affymetrix GCOS 1.4 software. The generated documents were analyzed according to the 'Affymetrix Statistical Algorithms Description Document'. Briefly, the raw data were subjected to processes including masking unusable data, background subtraction, probe values calculation, scaling, single chip analysis, and calculation of P-value. A probe-set was considered as expressed if the corresponding detection P-value was <0.04. Genes were considered to be differentially expressed if their ratio (patient/control) was higher or lower than 2-fold.

The gene functions were formatted for both gene ontologies (GO) and molecular function (9). The GO and molecular functions of the genes with 6-fold differential expression compared to controls were further analyzed by CapitalBio® Molecule Annotation System V3.0 (MAS3.0) (http://bioinfo.capitalbio.com/mas3/). The P-value was calculated according to a probability formula of hypergeometric distribution, reflecting the importance of the selected pathway or GO. The smaller the P-value, the higher its significance. The pathways were ranked in the order of P-value and the 10 most important ones were chosen for further analyses. Meanwhile, a Q-value corresponding to the P-value was calculated to evaluate the false discovery rate (FDR) of significant pathway and GO through screening by using a single P-value as cut-off. The smaller the Q-value, the lower the FDR.

All data are MIAME compliant and the raw data have been deposited in the GEO database (10) with the accession number of that, platform of GPL570, samples of GSM759883 and GSM759884, as well as series of GSE30643.

Quantitative RT-PCR (qRT-PCR). Prior to qRT-PCR, the RNA extracts were treated with a commercial RQ1 RNase-Free DNase (cat. #M6101; Promega) for 1 h at 37˚C according to the manufacturer's instructions. For cDNA synthesis, 2 μg of treated RNAs were mixed with the reagents in Reverse Transcription System (cat. #A3500; Promega). The real-time PCR was carried out on an ABI Prism 7900 sequencing detector, at the conditions of denaturing at 95˚C for 15 sec, annealing at 50˚C for 2 min and extension at 62˚C for 1 min, 40 cycles in total. β-actin gene was used as an internal control to normalize the expression levels of target mRNAs. The primers for each gene are shown in Table I.

Results

Global transcriptional profiling of the G114V gCJD patient. Following our previous studies on the G114V gCJD patient (7,8), we further investigated all the transcriptional patterns of the brain sample and compared them to those of normal brain RNA pool (control). To better understand the expression level of screened genes, we ranked them with the relative difference ratio using the following strategy: after single chip normalization, each probe set was marked as present (P) or absent (A)

Table I. Primers used for the real-time RT-PCR target genes.

	Gene ID	Sense primer	Antisense primer	Product length (bp)
Decreased genes	PHLDA2	ACAGCCTCTTCCAGCTATGG	GGTGGTGACGATGGTGAA	173
	HBB	ACGTGGATGAAGTTGGTGGT	CTCACTCAGTGTGGCAAAGGT	215
	NR4A2	ACCACTCTTCGGGAGAATACAG	ACAGGGGCATTTGGTACAAG	180
	CBLN4	CTGGGCACAGAACGACAC	AAGGCGACCTTGGAGTTG	144
Increased genes	ZNF396	TGGAAGAGGAAGAGCAGACC	CCTCAGCCAGAGATGACAAAG	167
	ZNF292	GAGCAGGAGAGGTTGAGTTG	AGATAAGGTCGGGCTTTAACA	257
	EIF5B	GACAGCACCAAGGATGACATT	GTTTTCTGTTGGCTTCACTGC	228
	UBE3A	GAGCAGCTGCAAAGCATCTA	CTTTCTTGGAGGGATGAGGAT	195

Table II. Significantly altered biological processes of gene ontology.

GO term	Count	P-value	Q-value	5 most up and downregulated genes, respectively[a]
GO:0006355 regulation of transcription, DNA-dependent	114	3.62E-72	2.60E-70	ATRX, CHD9, ZNF292, ZNF396, JMJD1C; *ZNF200, MEF2C, TBC1D9, ZMYM2, NR4A2*
GO:0007165 signal transduction	110	1.20E-49	6.34E-48	SYCP2, CPLX2, SLC5A3, GABRG1, BPTF; *SLC8A1, GRIN2A, ATP6V1B2, GRIN2A, GRIA4*
GO:0006350 transcription	106	3.72E-60	2.18E-58	PHF3, CHD9, ZNF292, ZNF396, JMJD1C; *ZNF200, BRWD1, MEF2C, ZMYM2, NR4A2*
GO:0007275 development	71	2.16E-31	6.11E-30	CSPP1, COL27A1, APC, TRAPPC2L, CD47; *PCDHA1, PCDH8, CD164, UCHL1, NELL1*
GO:0006810 transport	71	7.25E-29	1.94E-27	RNF130, DTNA, IL1RL1, PKN2, IL6ST; *RTN1, UCHL1, PENK, OR2L13, NR4A2*
GO:0006811 ion transport	68	3.08E-62	2.03E-60	TIMM8A, VEGFA, NAV1, MPPED2, FOSL2; *ITM2B, FGF13, UCHL1, NELL1, GAP43*
GO:0007155 cell adhesion	67	3.29E-59	1.86E-57	ASPH, JMJD1C, SYCP2, CPLX2, PLOD2; *PCYOX1, VAT1L, SQLE, KCNAB1, SRD5A1*
GO:0007399 nervous system development	57	5.56E-45	2.66E-43	ASPH, JMJD1C, SYCP2, CPLX2, PLOD2; *PCYOX1, VAT1L, SQLE, KCNAB1, SRD5A1*
GO:0015031 protein transport	53	5.92E-42	2.68E-40	TIMM8A, CEP290, RASEF, RASEF, HSP90B1; *ARF4, NSF, CADPS, CADPS, CADPS*
GO:0008152 metabolism	51	0.06	0.04	SFRS8, THOC2, PPIG, PRPF40A, ZRANB2; *MAGOH, LSM8, THOC4, SRPK2, RBM9*
GO:0008150 biological_process	50	1.00	0.58	GABRG1, SYN2, CTNNB1, MAPK12, MAPK11; *TAC1, SYT1, SYN2, SNAP25, SLC1A6*

[a]Downregulated genes are in italics.

according to the comparison to background noise. Probe sets marked with A in both the experimental sample and control were discarded. Thus, we found the differentially expressed genes based upon two criteria, i) present in sample but absent in another sample, or ii) with the gene expression level altered over 2-fold. The genes that met both conditions were considered DEGs. After purging the redundant probe sets reflecting same genes, a total of 8,774 genes were determined to be differentially expressed in G114V gCJD brains. Among them, nearly one-third (2,769) was upregulated and two-thirds (6,005) were downregulated. Due to the lack of sufficient sample/data from other gCJD patients, we were unable to make parallel experiments/comparisons to minimize the gene set of gCJD specific genes. Furthermore, we did not use data from sCJD (6) or prion-infected mice (5), as the different molecular background may have induced unpredictable bias.

According to the annotations of Affy-Chip, 8,494 of the 8,774 genes were either assigned biological functions or were

similar to genes with known functions, and 280 genes remain annotated as encoding hypothetical proteins. GO assignment determined these DEGs to be involved in 1,552 biological processes, with 819 molecular functions, and to be located in 368 cell components. In view of the significantly altered biological processes, 87 contained >10 DEGs. The predominantly altered processes covered the major basic cellular functions, including regulation of transcription, signal transduction, development and transport, oxidation reduction and apoptosis (Table II). Regarding the molecular functions, most DEGs were related to molecular (protein, nucleotide, ion) binding/interactions. The cellular component assignment showed that most functional genes were located in the membrane system (plasma membrane, mitochondria, endoplasmic reticulum). Since the sample was collected from the gCJD patient post-mortem, the transcriptional profile represents the terminal stage of the infected brain.

Identification of the most DEGs. According to the microarray results, the most upregulated genes included UBE3A and RBBP6, which are involved in the ubiquitin protein degradation system, suggesting that the ubiquitin-dependent catabolic processes are essential in the gCJD patient. ASPH was the second most highly expressed gene that plays an important role in calcium homeostasis. It is well known that destruction of calcium homeostasis is common in neurodegenerative diseases (11). On the contrary, the most downregulated genes included genes involved in iron ion binding (HBB), transcriptional regulation (NR4A2), signal transduction (OR2L13) and cell skeleton formation (NEFL) (Table III).

To evaluate the microarray results, we performed real-time PCR, targeting some specific genes from the brain of the G114V gCJD patient and the control RNA pool from the normal brain. Real-time PCR showed that the transcriptional levels of the downregulated genes HBB, CBLN4, PHLDA2 and NR4A2 from the microarray were markedly lower than those of the normal control, particularly PHLDA2 and NR4A2, which were >40-fold decreased and consistent with the microarray result. The upregulated genes EIF5B, UBE3A, ZNF396 and ZNF292 in the microarray were also significantly higher than the control in real-time PCR assay, particularly EIF5B, UBE3A and ZNF396 showing a >30-fold increase (Fig. 1). These findings indicate that the results of the microarray are reliable.

Involvement of significant pathways in G114V gCJD. To examine the changes of cell signaling pathways in the brain cortex of the G114V gCJD patient, the genes expressed at least 6-fold higher or lower than that of normal control were subsequently analyzed with the CapitalBio® Molecule Annotation System V3.0 (MAS 3.0) using KEGG pathways (12). In total, 169 different pathways with significant difference in expression ($P<0.05$) were identified. Briefly, 82 pathways were involved in metabolism, 28 in human diseases, 19 in organismal systems, 16 in environmental information processing, 14 in genetic information processing and 10 in cellular processes, according to the KEGG classification of functional pathways.

The 10 most altered pathways ranked in the order of P-value are summarized in Table IV. Most of the genes in these pathways were downregulated (Fig. 2). Notably, the first and the third most altered pathways were Alzheimer's disease (AD) and Parkinson's disease (PD). Within these two pathways, 31/34 genes and 27/28 genes were significantly downregulated in AD and PD pathways, respectively (Table IV). The downregulated genes related to these two pathways are involved in mitochondrial dysfunction, ER stress and apoptosis. These data suggest that G114V gCJD may share similar mechanisms to AD and PD.

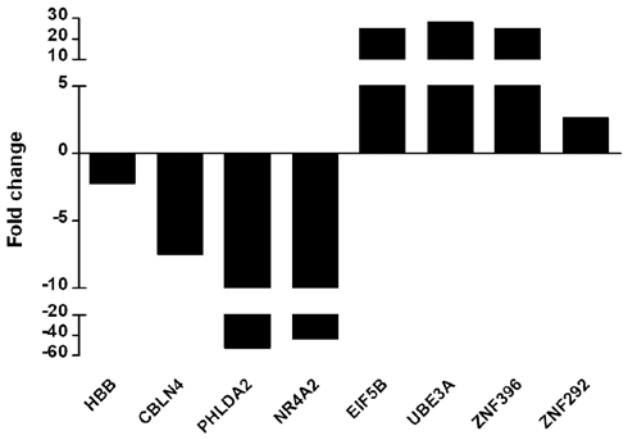

Figure 1. Confirmation of microarray results for the selected genes by real-time RT-PCR. Relative expression levels of the genes were indicated by the fold changes in expression level in G114V gCJD vs. control cases. The y-axis indicates fold changes and a negative value indicates downregulation.

Genes related to oxidative phosphorylation and purine metabolism were also significantly altered. Out of 30 differentially altered genes of involved in oxidative phosphorylation, 29 were downregulated, including NADH dehydrogenase, succinate dehydrogenase, cytochrome *c* reductase, cytochrome *c* oxidase and F-type ATPase (Fig. 2). Regarding the purine metabolism pathway, all 24 altered genes were downregulated, including adenylosuccinate lyase, RNA polymerase II and some phosphodiesterases (Fig. 2). These observations indicate that there is a severe failure in the mitochondria and a severe dysfunction of cell metabolism at the terminal stage.

Two pathways related to the cytoskeleton were also markedly downregulated; 29/32 altered genes involved in the regulation of actin cytoskeleton were significantly downregulated. All 17 affected genes related to pathogenic *Escherichia coli* infection were downregulated; among them some gene products were cell structure proteins, i.e. CDC42 and tubulin. Additionally, other possible severely disrupted pathways included those related to gap junctions (17/20 DEGs downregulated), which are involved in direct communication between the cytosolic compartments of adjacent cells and the pathway of axon guidance (24/24 DEGs downregulated), which helps axons extend to their correct targets. The downregulation of these two pathways suggests that there is damage to cell communication and neuronal development in the G114V gCJD brain.

Among the 10 most affected pathways, the mitogen-activated protein kinase (MAPK) signaling pathway was the only one related to environmental signaling processing. The processes seemed to be markedly repressed as well, with 33/35 altered genes being downregulated, including kinases

Table III. Most differentially expressed genes of the microarray data.

Gene	Description	Ratio	Gene Ontology		
			Biological process	Cellular component	Molecular function
UBE3A	Ubiquitin protein ligase E3A	75.71	Protein modification process; proteolysis; ubiquitin-dependent protein catabolic process; brain development; modification-dependent protein catabolic process; interspecies interaction between organisms	Intracellular; nucleus; cytosol; protein complex	Ubiquitin-protein ligase activity; protein binding; acid-amino acid ligase activity
ASPH	Aspartate β-hydroxylase	72.30	Muscle contraction; peptidyl-amino acid modification; oxidation reduction	Integral to membrane; integral to endoplasmic reticulum membrane	Peptide-aspartate β-dioxygenase activity; structural molecule activity; iron ion binding; calcium ion binding; structural constituent of muscle; electron carrier activity; oxidoreductase activity
CCDC88A	Coiled-coil domain containing 88A	47.85	Regulation of protein amino acid phosphorylation; regulation of DNA replication; membrane organization; cell migration; lamellipodium assembly; activation of protein kinase B activity; regulation of actin cytoskeleton organization; regulation of cell proliferation	Cytoplasm; endoplasmic reticulum; Golgi apparatus; cytosol; plasma membrane; membrane; lamellipodium; cytoplasmic vesicle; cell projection	Actin binding; microtubule binding; phosphoinositide binding; protein homodimerization activity; protein kinase B binding
RBBP6	Retinoblastoma binding protein 6	36.45	Protein ubiquitination	Ubiquitin ligase complex; nucleus	Nucleic acid binding; ubiquitin-protein ligase activity; zinc ion binding
LOC643187	Hypothetical LOC643187	30.62	N/A	N/A	N/A
ANKRD12	Ankyrin repeat domain 12	30.27	N/A	Nucleus; ribosome	N/A
LOC554203	Alanyl-tRNA synthetase domain containing 1 pseudogene	29.83	N/A	N/A	N/A
ANKRD36	Ankyrin repeat domain 36	25.71	N/A	N/A	N/A
PHF3	PHD finger protein 3	25.30	Transcription; multicellular organismal development	Nucleus	Protein binding; zinc ion binding
EIF5B	Eukaryotic translation initiation factor 5B	24.24	Translation; regulation of translational initiation	Cytoplasm	Nucleotide binding; translation initiation factor activity; GTPase activity; protein binding; GTP binding
HBB	Hemoglobin, β	0.004	Regulation of blood pressure; oxygen transport; positive regulation of nitric oxide biosynthetic process; regulation of blood vessel size	Hemoglobin complex	Oxygen transporter activity; iron ion binding; oxygen binding; hemoglobin binding

Table III. Continued.

Gene	Description	Ratio	Gene Ontology		
			Biological process	Cellular component	Molecular function
TSPYL1	TSPY-like 1	0.006	Nucleosome assembly	Intracellular; nucleus	N/A
GAP43	Growth associated protein 43	0.009	Activation of protein kinase C activity by GPCR protein signaling pathway; nervous system development; response to wounding; glial cell differentiation; axon choice point recognition; regulation of growth; tissue regeneration; cell fate commitment	Plasma membrane; membrane; cell junction; axon; cell projection; synapse	Calmodulin binding
NR4A2	Nuclear receptor, subfamily 4, group A, member 2	0.009	DNA-dependent regulation of transcription; signal transduction; cellular response to extracellular stimulus; respose to protein stimulus	Nucleus	Transcription factor activity; steroid hormone receptor activity; zinc ion binding; sequence-specific DNA binding
PHLDA2	Pleckstrin homology-like domain, family A, member 2	0.009	Apoptosis; organ morphogenesis	Cytoplasm; membrane	N/A
OR2L13	Olfactory receptor, family 2, subfamily L, member 13	0.01	Signal transduction; GPCR protein signaling pathway; sensory perception of smell; response to stimulus	Plasma membrane; membrane; integral to membrane	Signal transducer activity; olfactory receptor activity
NEFL	Neurofilament, light polypeptide	0.01	Anterograde axon cargo transport; retrograde axon cargo transport; axon regeneration in the peripheral nervous system; axon transport of mitochondrion; regulation of axon diameter; neurofilament bundle assembly; locomotion; negative regulation of neuron apoptosis; intermediate filament bundle assembly; neuron projection morphogenesis; positive regulation of axonogenesis; neuromuscular process controlling balance; neurofilament cytoskeleton organization	Intermediate filament; neurofilament; axon; TSC1-TSC2 complex	Structural molecule activity; structural constituent of cytoskeleton; protein C-terminus binding; identical protein binding
C11orf87	Chromosome 11 open reading frame 87	0.018	N/A	Integral to membrane	N/A
CBLN4	Cerebellin 4 precursor	0.019	N/A	Extracellular region; cell junction; synapse	N/A
CD200	CD200 molecule	0.019	N/A	Integral to plasma membrane; integral to membrane	Protein binding

Table IV. The 10 most significantly regulated pathways deduced from the microarray data.

Pathway	Count	P-value	Q-value
Alzheimer's disease	34	1.26E-17	1.79E-16
Oxidative phosphorylation	30	3.42E-17	4.60E-16
Parkinson's disease	28	1.40E-15	1.47E-14
Regulation of actin cytoskeleton	32	2.97E-13	1.84E-12
Pathogenic *Escherichia coli* infection	17	4.20E-13	2.45E-12
MAPK signaling pathway	35	1.67E-12	8.40E-12
Axon guidance	24	1.79E-12	8.83E-12
Gap junction	20	6.58E-12	3.01E-11
Proteasome	15	8.43E-12	3.78E-11
Purine metabolism	24	5.64E-11	2.20E-10

(MAPK1, MAPK1, MAP2K1, MAP2K4, PRKCB, PAK1 and STK4), phosphatases (DUSP4, DUSP5, DUSP6, PPP3CA and PPP3CB) and some regulatory factors (FGF13, FGF14, MEF2C and RASGRF2) (Fig. 2). These genes were distributed in the three sub-pathways, classical MAP kinase pathway, JNK and p38 MAP kinase pathway, and extracellular-regulated kinase 5 (ERK5) pathway. This indicates that the local information processing in the brain of the gCJD patient was severely impaired.

The transcriptional pattern of important prion disease associated genes. Our previous study demonstrated large amounts of PrP^{Sc} deposits and severe gliosis in the cortex regions of this G114V gCJD patient, while the transcription levels of *PRNP* did not vary as much as in the PrP^{Sc} deposit among 10 different regions (8). Furthermore, microarray data showed no difference in *PRNP* transcription between the patient's brain and normal control, even slightly downregulated in the patient's brain with several *PRNP* probes, possibly indicating deposits of PrP^{Sc} in brains do not lead to enhancing the *PRNP* transcription. The transcriptional level of the GFAP gene in the patient was ~2-fold increased relative to that of the control, highlighting an active gliosis. Nevertheless, a spectrum of neuronal biomarkers was downregulated in the patient's brain, such as NSE (7.25-fold), tubulin-β III (3.88-fold), MAP2 (8.13-fold), NF-M (38.46-fold), NF-H (12.35-fold) and NF subunit NF-L (27.78-fold), demonstrating severe neuron loss. These data are consistent with the pathological characteristics of G114V gCJD.

Discussion

In the present study, we analyzed the global expression patterns in the parietal cortex of a G114V gCJD patient with a commercial gene chip containing 47,000 transcripts. This is the highest-capacity approach to gene expression analysis used in human prion disease thus far. After purging the redundant transcripts, we identified 2,769 upregulated and 6,005 downregulated genes. Further qRT-PCRs for several differentially expressed genes confirmed the results of the microarray. Notably, more downregulated genes in the brain of G114V gCJD are consistent with the results of a previous study on sporadic CJD with a relatively lower throughput microarray (18,000 transcripts), in which 275 genes out of 287 differentially expressed genes were downregulated (6).

In line with the observations of the pathological abnormalities in the G114V gCJD patient (8,13), the transcriptional level of the GFAP gene associated with gliosis is increased and a series of genes associated with neurons are decreased. Although the brain tissues are severely damaged pathologically, the expression levels of prion protein gene *PRNP* do not differ distinctly compared with those of normal control, which is in accordance not only with the data of *PRNP* transcription in this patient with qRT-PCR, but also with the previous microarray findings in the sCJD patients (6), mice infected with scrapie or CJD agents (14) and cattle infected with the BSE agent (15). Maintenance of active transcription of the *PRNP* gene in CNS tissues at the terminal stage of human and animal prion diseases may indicate a special environment that facilitates the replication of prion agents locally by supplying enough PrP^{C} as the substrates for PrP^{Sc} replication.

The most differentially expressed genes in G114V gCJD seem to be involved in multiple cell processes, such as regulation of transcription, ion transport, cell adhesion, signal transduction, nervous system development, oxidation reduction, protein transport, RNA splicing and synaptic transmission. In the brains of naturally-occurring or experimental animal and human TSEs, as well as in some prion infected cell lines (5,6,15-17), abnormal alterations in ion transportation, transcription, cell adhesion, signal transduction and synaptic transmission have been repeatedly observed. Numerous differentially expressed genes involved in different cell processes or networks in brain tissues of this G114V gCJD patient reflect an extensive brain dysfunction at the final period of the disease.

Based on the classification of the KEGG database, 169 different pathways were significantly altered in the brain of the patient with G114V gCJD. Most of the differentially expressed genes in the 10 most significantly altered pathways were downregulated, revealing a deeply suppressed expression status of the relevant functions. Two metabolic pathways, oxidative phosphorylation and purine metabolism, were markedly repressed in our study. In the oxidative phosphorylation pathway, the expression of several key elements, such as NADH dehydrogenase, succinate dehydrogenase, cytochrome *c* reductase,

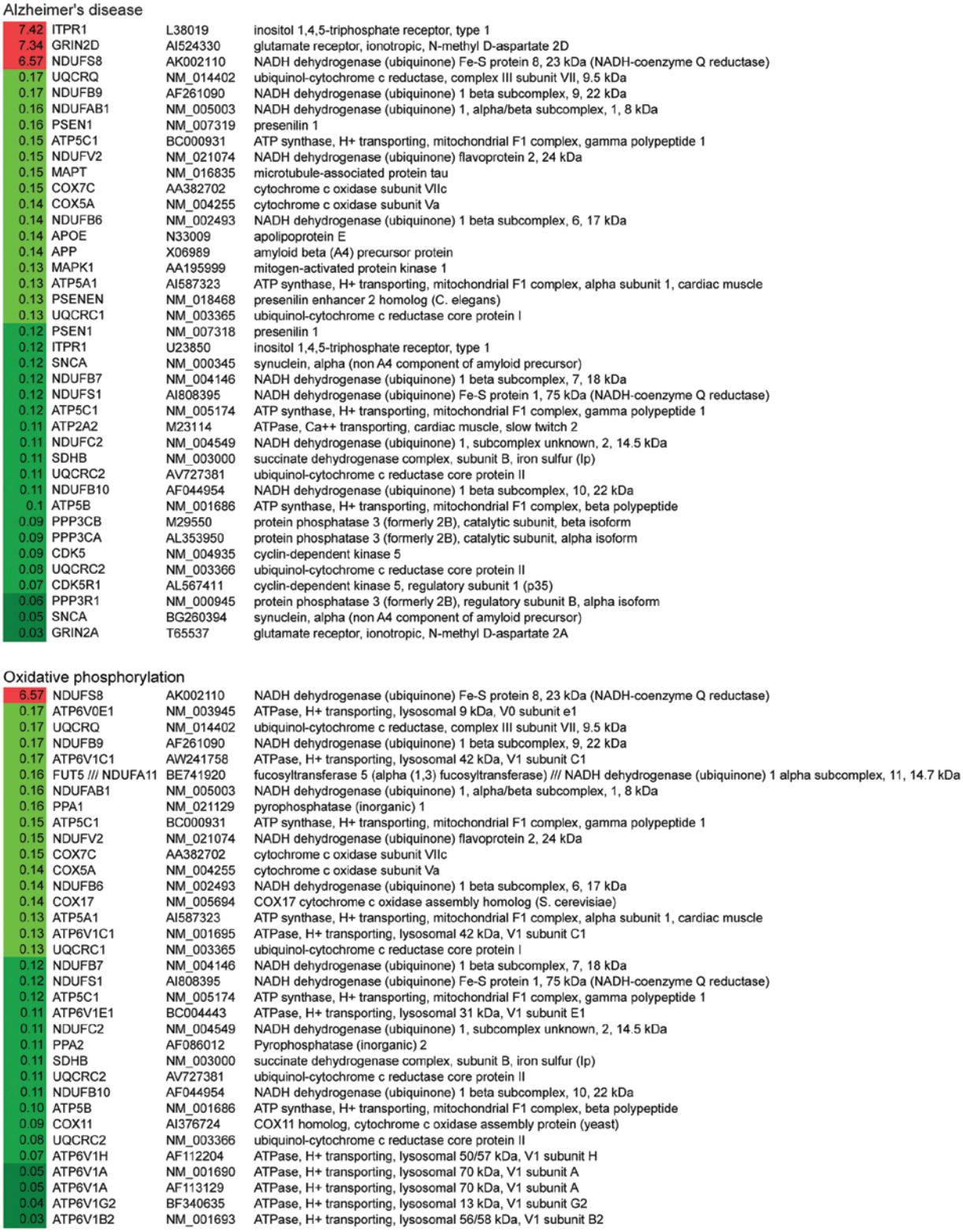

Figure 2. The 10 most altered pathways and the differentially expressed genes in them. The red color represents the upregulated genes and the green indicates downregulated ones. The gene symbols, RefSeq transcript ID, and gene titles of differentially expressed genes in each pathway are listed on the right. The altered ratios corresponding to various genes involved in pathways are indicated on the left.

cytochrome *c* oxidase and F-type ATPase were decreased. This result is in accordance with previous studies by both microarray (5) and proteomics (18), reflecting a complete failure of mitochondria. Purine metabolism includes the biological synthesis, degradation and salvation of purines, an essential component of nucleotides (19). Abnormality in this pathway has not previously been observed in the prion-infected cells, or human and animal TSEs. Besides, the pathway of cellular proteasome in the brain of this gCJD case is significantly involved, in which various proteasome subunits are downregulated. The dysfunc-

Parkinson's disease

6.57	NDUFS8	AK002110	NADH dehydrogenase (ubiquinone) Fe-S protein 8, 23 kDa (NADH-coenzyme Q reductase)
0.17	PPID	AI014573	peptidylprolyl isomerase D
0.17	UQCRQ	NM_014402	ubiquinol-cytochrome c reductase, complex III subunit VII, 9.5 kDa
0.17	NDUFB9	AF261090	NADH dehydrogenase (ubiquinone) 1 beta subcomplex, 9, 22 kDa
0.16	NDUFAB1	NM_005003	NADH dehydrogenase (ubiquinone) 1, alpha/beta subcomplex, 1, 8 kDa
0.15	ATP5C1	BC000931	ATP synthase, H+ transporting, mitochondrial F1 complex, gamma polypeptide 1
0.15	NDUFV2	NM_021074	NADH dehydrogenase (ubiquinone) flavoprotein 2, 24 kDa
0.15	UBE2G1	AW299555	ubiquitin-conjugating enzyme E2G 1 (UBC7 homolog, yeast)
0.15	COX7C	AA382702	cytochrome c oxidase subunit VIIc
0.14	COX5A	NM_004255	cytochrome c oxidase subunit Va
0.14	NDUFB6	NM_002493	NADH dehydrogenase (ubiquinone) 1 beta subcomplex, 6, 17 kDa
0.14	HTRA2	NM_013247	HtrA serine peptidase 2
0.13	ATP5A1	AI587323	ATP synthase, H+ transporting, mitochondrial F1 complex, alpha subunit 1, cardiac muscle
0.13	UQCRC1	NM_003365	ubiquinol-cytochrome c reductase core protein I
0.12	UBE2L3	BG531983	ubiquitin-conjugating enzyme E2L 3
0.12	SLC25A4	NM_001151	solute carrier family 25 (mitochondrial carrier; adenine nucleotide translocator), member 4
0.12	SNCA	NM_000345	synuclein, alpha (non A4 component of amyloid precursor)
0.12	NDUFB7	NM_004146	NADH dehydrogenase (ubiquinone) 1 beta subcomplex, 7, 18 kDa
0.12	ATP5C1	NM_005174	ATP synthase, H+ transporting, mitochondrial F1 complex, gamma polypeptide 1
0.11	NDUFC2	NM_004549	NADH dehydrogenase (ubiquinone) 1, subcomplex unknown, 2, 14.5 kDa
0.11	SDHB	NM_003000	succinate dehydrogenase complex, subunit B, iron sulfur (Ip)
0.11	UQCRC2	AV727381	ubiquinol-cytochrome c reductase core protein II
0.11	NDUFB10	AF044954	NADH dehydrogenase (ubiquinone) 1 beta subcomplex, 10, 22 kDa
0.10	ATP5B	NM_001686	ATP synthase, H+ transporting, mitochondrial F1 complex, beta polypeptide
0.10	VDAC3	U90943	voltage-dependent anion channel 3
0.09	UBE2G1	BC002775	ubiquitin-conjugating enzyme E2G 1 (UBC7 homolog, yeast)
0.08	VDAC1	AL515918	voltage-dependent anion channel 1
0.08	UQCRC2	NM_003366	ubiquinol-cytochrome c reductase core protein II
0.05	GPR37	U87460	G protein-coupled receptor 37 (endothelin receptor type B-like)
0.05	SNCA	BG260394	synuclein, alpha (non A4 component of amyloid precursor)
0.02	UCHL1	NM_004181	ubiquitin carboxyl-terminal esterase L1 (ubiquitin thiolesterase)

Regulation of actin cytoskeleton

9.47	PPP1R12A	BE737620	protein phosphatase 1, regulatory (inhibitor) subunit 12A
6.17	SOS2	BF692958	son of sevenless homolog 2 (Drosophila)
6.05	APC	M74088	adenomatous polyposis coli
0.16	PTK2	AA912743	PTK2 protein tyrosine kinase 2
0.15	TIAM2	AI094945	T-cell lymphoma invasion and metastasis 2
0.15	ACTN2	AU146889	actinin, alpha 2
0.14	PIP4K2C	NM_024779	phosphatidylinositol-5-phosphate 4-kinase, type II, gamma
0.14	ARPC2	AF279893	actin related protein 2/3 complex, subunit 2, 34 kDa
0.14	RHOA	AF498970	ras homolog gene family, member A
0.13	MAPK1	AA195999	mitogen-activated protein kinase 1
0.13	WASL	BE504979	Wiskott-Aldrich syndrome-like
0.13	MYH10	AK026977	myosin, heavy chain 10, non-muscle
0.13	FGF14	BE549937	fibroblast growth factor 14
0.13	ARHGEF7	AI040887	Rho guanine nucleotide exchange factor (GEF) 7
0.13	TIAM1	U90902	T-cell lymphoma invasion and metastasis 1
0.12	CDC42	N92917	Cell division cycle 42 (GTP binding protein, 25 kDa)
0.12	CDC42	N92917	Cell division cycle 42 (GTP binding protein, 25 kDa)
0.12	GSN	NM_000177	gelsolin (amyloidosis, Finnish type)
0.11	PIP5K1B	NM_003558	phosphatidylinositol-4-phosphate 5-kinase, type I, beta
0.11	NCKAP1	NM_013436	NCK-associated protein 1
0.11	ARPC3	AF004561	actin related protein 2/3 complex, subunit 3, 21 kDa
0.11	CFL1	D00682	cofilin 1 (non-muscle)
0.10	ARPC1A	NM_006409	actin related protein 2/3 complex, subunit 1A, 41 kDa
0.10	WASL	AL523820	Wiskott-Aldrich syndrome-like
0.10	WASF1	NM_003931	WAS protein family, member 1
0.10	FGFR2	NM_022975	fibroblast growth factor receptor 2
0.09	FGF14	NM_004115	fibroblast growth factor 14
0.09	MAP2K1	AI571419	mitogen-activated protein kinase kinase 1
0.09	ITGAM	NM_000632	integrin, alpha M (complement component 3 receptor 3 subunit)
0.09	ARPC5L	AU158936	actin related protein 2/3 complex, subunit 5-like
0.07	RDX	AI051769	radixin
0.07	PAK1	AU147145	p21 protein (Cdc42/Rac)-activated kinase 1
0.06	ACTN2	H16245	actinin, alpha 2
0.05	CDC42	R37664	cell division cycle 42 (GTP binding protein, 25 kDa)
0.04	CDC42	M35543	cell division cycle 42 (GTP binding protein, 25 kDa)
0.03	FGF13	NM_004114	fibroblast growth factor 13
0.03	ARHGEF7	AI990366	Rho guanine nucleotide exchange factor (GEF) 7

Figure 2. Continued.

tion of the cellular proteasome system is often noticed in several neurodegenerative disorders (18), including prion disease (20). The disability of protein degradation, especially in clearance of misfolded protein, may contribute to the accumulation of PrP^{Sc} in brain tissues.

It has been repeatedly observed that the cytoskeleton and microtubule are severely destroyed in the brain of prion disease (21-23). In our study, the pathway of regulation of actin cytoskeleton and the pathway involved in the expressions of cell structure proteins, such as CDC42 and tubulin, were clearly suppressed. Reduction of expression levels of those genes results in rearrangement of the cytoskeleton, disruption of barrier function and an increase in monolayer permeability.

The MAPK cascade is a highly conserved pathway involved in various cellular functions, including cell proliferation, differentiation and migration. Our microarray experiment illustrated the increased expression of p38 MAP kinase and nuclear factor-κB (NF-κB) in the brain of gCJD. The increase

Pathogenic Escherichia coli infection

0.16	TUBB2C	BC004188	tubulin, beta 2C
0.16	TUBA1B	BC006481	tubulin, alpha 1b
0.16	TUBA1C	BC005946	tubulin, alpha 1c
0.15	TUBA1B	BE300252	tubulin, alpha 1b
0.15	TUBA1B	AL581768	tubulin, alpha 1b
0.15	TUBA1C	BC004949	tubulin, alpha 1c
0.15	TUBA1B	BC006379	tubulin, alpha 1b
0.15	CTNNB1	AB062292	catenin (cadherin-associated protein), beta 1, 88 kDa
0.13	TUBB2A	NM_001069	tubulin, beta 2A
0.13	WASL	BE504979	Wiskott-Aldrich syndrome-like
0.13	TUBB2A /// TUBB2B	BF971587	tubulin, beta 2A /// tubulin, beta 2B
0.13	TUBB	BC001002	tubulin, beta
0.12	CDC42	N92917	Cell division cycle 42 (GTP binding protein, 25 kDa)
0.10	TUBB4	AL567012	tubulin, beta 4
0.10	WASL	AL523820	Wiskott-Aldrich syndrome-like
0.09	ARPC5L	AU158936	actin related protein 2/3 complex, subunit 5-like
0.09	TUBB	BC005838	tubulin, beta
0.09	TUBA3C	L11645	tubulin, alpha 3c
0.08	TUBB	AF141349	tubulin, beta
0.06	YWHAZ	NM_003406	tyrosine 3-monooxygenase/tryptophan 5-monooxygenase activation protein, zeta polypeptide
0.06	YWHAZ	BC003623	tyrosine 3-monooxygenase/tryptophan 5-monooxygenase activation protein, zeta polypeptide
0.06	TUBA4A	AL565074	tubulin, alpha 4a
0.06	TUBA3D	K03460	tubulin, alpha 3d
0.05	CDC42	R37664	cell division cycle 42 (GTP binding protein, 25 kDa)
0.04	CDC42	M35543	cell division cycle 42 (GTP binding protein, 25 kDa)

MAPK signaling pathway

9.44	EVI1	BE466525	ecotropic viral integration site 1
6.17	SOS2	BF692958	son of sevenless homolog 2 (Drosophila)
0.16	DUSP6	BC003143	dual specificity phosphatase 6
0.16	DUSP5	U16996	dual specificity phosphatase 5
0.15	MAPT	NM_016835	microtubule-associated protein tau
0.15	RASA1	NM_002890	RAS p21 protein activator (GTPase activating protein) 1
0.15	MAPK9	AI808345	mitogen-activated protein kinase 9
0.15	DUSP4	NM_001394	dual specificity phosphatase 4
0.13	MAPK1	AA195999	mitogen-activated protein kinase 1
0.13	FGF14	BE549937	fibroblast growth factor 14
0.13	HSPA2	U56725	heat shock 70 kDa protein 2
0.13	STMN1	NM_005563	stathmin 1
0.12	CDC42	N92917	Cell division cycle 42 (GTP binding protein, 25 kDa)
0.12	MEF2C	AL536517	myocyte enhancer factor 2C
0.12	STK4	BC005231	serine/threonine kinase 4
0.11	HSPA8	AB034951	heat shock 70kDa protein 8
0.10	PRKCB	M13975	protein kinase C, beta
0.10	FGFR2	NM_022975	fibroblast growth factor receptor 2
0.09	PPP3CB	M29550	protein phosphatase 3 (formerly 2B), catalytic subunit, beta isoform
0.09	FGF14	NM_004115	fibroblast growth factor 14
0.09	MAP2K1	AI571419	mitogen-activated protein kinase kinase 1
0.09	CACNB2	AI040163	calcium channel, voltage-dependent, beta 2 subunit
0.09	PPP3CA	AL353950	protein phosphatase 3 (formerly 2B), catalytic subunit, alpha isoform
0.09	MAPK9	W37431	mitogen-activated protein kinase 9
0.09	MAP2K4	NM_003010	mitogen-activated protein kinase kinase 4
0.08	RASGRF2	AI912976	Ras protein-specific guanine nucleotide-releasing factor 2
0.07	CACNA1E	R15004	calcium channel, voltage-dependent, R type, alpha 1E subunit
0.07	PAK1	AU147145	p21 protein (Cdc42/Rac)-activated kinase 1
0.06	CACNA2D3	NM_018398	calcium channel, voltage-dependent, alpha 2/delta subunit 3
0.06	HSPA1A /// HSPA1B	NM_005346	heat shock 70 kDa protein 1A/// heat shock 70 kDa protein 1B
0.06	PPP3R1	NM_000945	protein phosphatase 3 (formerly 2B), regulatory subunit B, alpha isoform
0.06	FOS	BC004490	v-fos FBJ murine osteosarcoma viral oncogene homolog
0.06	NF1	AK024873	neurofibromin 1
0.05	HSPA1A /// HSPA1B	NM_005345	heat shock 70 kDa protein 1A/// heat shock 70 kDa protein 1B
0.05	MEF2C	N22468	myocyte enhancer factor 2C
0.05	RASA1	M23612	RAS p21 protein activator (GTPase activating protein) 1
0.05	CDC42	R37664	cell division cycle 42 (GTP binding protein, 25 kDa)
0.05	MAP2K4	AA810268	mitogen-activated protein kinase kinase 4
0.04	CDC42	M35543	cell division cycle 42 (GTP binding protein, 25 kDa)
0.03	FGF13	NM_004114	fibroblast growth factor 13
0.03	PRKCB	NM_002738	protein kinase C, beta

Figure 2. Continued.

of those two factors has been reported in cells treated with the peptide PrP106-126. PrP106-126 has been demonstrated to activate p38 MAP kinase in human microglia accompanied by upregulation of NF-κB (24), and to induce a p38 MAP kinase-dependent apoptosis in SH-SY5Y neuroblastoma cells independently from the amyloid fibril formation (25). The decrease of ERK in our microarray is also in line with the observation that PrP fragment (aa 90-231) activates p38 MAP kinase by inhibiting the activation of extracellular-regulated kinases 1/2 (ERK1/2), followed by the caspase-3-dependent cell apoptosis in SH-SY5Y cells (26).

Genes involved in axon guidance and gap junctions, which are critical for cell communication and cell development, are rarely investigated in prion diseases. Axon guidance is a subfield of neural development concerning the process by which neurons send out axons to reach the correct targets. Its role in prion disease is rarely described, until recently a group performed systematical analyses on the gene changes

Axon guidance

0.16	NTN4	AF278532	netrin 4
0.16	PTK2	AA912743	PTK2 protein tyrosine kinase 2
0.15	RASA1	NM_002890	RAS p21 protein activator (GTPase activating protein) 1
0.14	SEMA4D	NM_006378	sema domain, immunoglobulin domain (Ig), transmembrane domain (TM) and short cytoplasmic domain, (semaphorin) 4D
0.14	RHOA	AF498970	ras homolog gene family, member A
0.13	MAPK1	AA195999	mitogen-activated protein kinase 1
0.12	CDC42	N92917	Cell division cycle 42 (GTP binding protein, 25 kDa)
0.12	SEMA5A	BG109855	sema domain, seven thrombospondin repeats (type 1 and type 1-like), transmembrane domain and short cytoplasmic domain, (semaphorin) 5A
0.11	CFL1	D00682	cofilin 1 (non-muscle)
0.10	SLIT1	AB011537	slit homolog 1 (Drosophila)
0.09	PPP3CB	M29550	protein phosphatase 3 (formerly 2B), catalytic subunit, beta isoform
0.09	PPP3CA	AL353950	protein phosphatase 3 (formerly 2B), catalytic subunit, alpha isoform
0.09	ROBO2	AB046788	roundabout, axon guidance receptor, homolog 2 (Drosophila)
0.09	SEMA3C	NM_006379	sema domain, immunoglobulin domain (Ig), short basic domain, secreted, (semaphorin) 3C
0.09	CDK5	NM_004935	cyclin-dependent kinase 5
0.08	GNAI1	AU153866	guanine nucleotide binding protein (G protein), alpha inhibiting activity polypeptide 1
0.08	PLXNC1	AF035307	plexin C1
0.08	EFNA5	AK025909	Ephrin-A5
0.07	PAK1	AU147145	p21 protein (Cdc42/Rac)-activated kinase 1
0.07	CXCR4	AJ224869	chemokine (C-X-C motif) receptor 4
0.06	EPHA4	AI799018	EPH receptor A4
0.06	PPP3R1	NM_000945	protein phosphatase 3 (formerly 2B), regulatory subunit B, alpha isoform
0.05	RASA1	M23612	RAS p21 protein activator (GTPase activating protein) 1
0.05	CDC42	R37664	cell division cycle 42 (GTP binding protein, 25 kDa)
0.04	CDC42	M35543	cell division cycle 42 (GTP binding protein, 25 kDa)
0.03	GNAI1	AL049933	guanine nucleotide binding protein (G protein), alpha inhibiting activity polypeptide 1

Gap junction

9.27	ADRB1	NM_000684	adrenergic, beta-1-, receptor
7.42	ITPR1	L38019	inositol 1,4,5-triphosphate receptor, type 1
6.17	SOS2	BF692958	son of sevenless homolog 2 (Drosophila)
0.16	TUBB2C	BC004188	tubulin, beta 2C
0.16	TUBA1B	BC006481	tubulin, alpha 1b
0.16	TUBA1C	BC005946	tubulin, alpha 1c
0.15	TUBA1B	BE300252	tubulin, alpha 1b
0.15	TUBA1B	AL581768	tubulin, alpha 1b
0.15	TUBA1C	BC004949	tubulin, alpha 1c
0.15	TUBA1B	BC006379	tubulin, alpha 1b
0.13	MAPK1	AA195999	mitogen-activated protein kinase 1
0.13	TUBB2A	NM_001069	tubulin, beta 2A
0.13	TUBB2A /// TUBB2B	BF971587	tubulin, beta 2A /// tubulin, beta 2B
0.13	GNAS	AA401492	GNAS complex locus
0.13	TUBB	BC001002	tubulin, beta
0.12	ITPR1	U23850	inositol 1,4,5-triphosphate receptor, type 1
0.10	TUBB4	AL567012	tubulin, beta 4
0.10	PRKCB	M13975	protein kinase C, beta
0.09	MAP2K1	AI571419	mitogen-activated protein kinase kinase 1
0.09	TUBB	BC005838	tubulin, beta
0.09	GRM1	NM_000838	glutamate receptor, metabotropic 1
0.09	TUBA3C	L11645	tubulin, alpha 3c
0.08	TUBB	AF141349	tubulin, beta
0.06	TUBA4A	AL565074	tubulin, alpha 4a
0.06	TUBA3D	K03460	tubulin, alpha 3d
0.05	GUCY1B3	W93728	guanylate cyclase 1, soluble, beta 3
0.03	GNAI1	AL049933	guanine nucleotide binding protein (G protein), alpha inhibiting activity polypeptide 1
0.03	PRKCB	NM_002738	protein kinase C, beta

Figure 2. Continued.

in the brains of eight mouse adapted-prion strains throughout the progression of the diseases. Axon guidance disturbance was found in the mice with shorter incubation times (5). Gap junctions are involved in direct communication between the cytosolic compartments of adjacent cells. Apart from the changes of MAPK associated genes, some receptors of monoamines and other biogenic amine neurotransmitters, such as β-1 adrenergic receptor (ADRB1), dopamine receptor D2 (DRD2), 5-hydroxytryptamine (serotonin) receptor 2 (HTR2) and mGluR are suppressed, resulting in abnormal regulation of the expressions of the genes downstream and subsequently inducing the dysfunction of calcium signaling pathway and transportation of other biological masses.

The most significantly altered pathways in human diseases in the brain of the G114V gCJD patient are those of AD and PD, strongly indicating that G114V gCJD shares the similar gene expression profiles as these two neurodegenerative diseases. Among these two pathways, cell death induced by changes of oxidative phosphorylation in the mitochondria is a critical factor for neuron loss in AD and PD (18,27). In G114V gCJD, distinct impediment of oxidation phosphorylation is also observed. This includes abnormal phosphorylation, ATP depletion, collapse of mitochondrial membrane potential, increase of reactive oxygen species (ROS). Moreover, reduction of the expression of the relevant genes in this gCJD case highlight the presence of the similar ER stress-induced cell

Proteasome

0.17	PSMC3	AL545523	proteasome (prosome, macropain) 26S subunit, ATPase, 3
0.16	PSMC2	NM_002803	proteasome (prosome, macropain) 26S subunit, ATPase, 2
0.15	PSMA5	NM_002790	proteasome (prosome, macropain) subunit, alpha type, 5
0.14	PSMD8	NM_002812	proteasome (prosome, macropain) 26S subunit, non-ATPase, 8
0.13	PSMD6	NM_014814	proteasome (prosome, macropain) 26S subunit, non-ATPase, 6
0.13	PSMB4	NM_002796	proteasome (prosome, macropain) subunit, beta type, 4
0.13	PSMB3	NM_002795	proteasome (prosome, macropain) subunit, beta type, 3
0.13	PSMB6	BC000835	proteasome (prosome, macropain) subunit, beta type, 6
0.13	PSMB2	NM_002794	proteasome (prosome, macropain) subunit, beta type, 2
0.12	PSMB7	NM_002799	proteasome (prosome, macropain) subunit, beta type, 7
0.11	PSMC4	NM_006503	proteasome (prosome, macropain) 26S subunit, ATPase, 4
0.11	PSMA1	M64992	proteasome (prosome, macropain) subunit, alpha type, 1
0.09	PSMB1	NM_002793	proteasome (prosome, macropain) subunit, beta type, 1
0.09	PSMA1	NM_002786	proteasome (prosome, macropain) subunit, alpha type, 1
0.07	PSMA1	BC005932	proteasome (prosome, macropain) subunit, alpha type, 1
0.05	PSMD12	NM_002816	proteasome (prosome, macropain) 26S subunit, non-ATPase, 12

Purine metabolism

0.17	PRPS1	NM_002764	phosphoribosyl pyrophosphate synthetase 1
0.16	PAPSS1	AF033026	3'-phosphoadenosine 5'-phosphosulfate synthase 1
0.15	PDE6D	AJ001626	phosphodiesterase 6D, cGMP-specific, rod, delta
0.15	POLE3	BC004170	polymerase (DNA directed), epsilon 3 (p17 subunit)
0.14	POLR2E	AI554759	polymerase (RNA) II (DNA directed) polypeptide E, 25 kDa
0.14	POLR2B	BE614461	polymerase (RNA) II (DNA directed) polypeptide B, 140 kDa
0.14	POLR2K	NM_005034	polymerase (RNA) II (DNA directed) polypeptide K, 7.0 kDa
0.13	PRPS2	AI392908	Phosphoribosyl pyrophosphate synthetase 2
0.12	DCK	NM_000788	deoxycytidine kinase
0.12	POLR3K	NM_016310	polymerase (RNA) III (DNA directed) polypeptide K, 12.3 kDa
0.12	ENTPD3	NM_001248	ectonucleoside triphosphate diphosphohydrolase 3
0.11	PRPS1	BC001605	phosphoribosyl pyrophosphate synthetase 1
0.11	ADSL	AF067854	adenylosuccinate lyase
0.11	DGUOK	NM_001929	deoxyguanosine kinase
0.10	PDE10A	AI143879	phosphodiesterase 10A
0.10	ADSS	AA628948	adenylosuccinate synthase
0.08	PDE8B	AB085825	phosphodiesterase 8B
0.07	AK5	NM_012093	adenylate kinase 5
0.06	GDA	AF019638	guanine deaminase
0.06	NME1	NM_000269	non-metastatic cells 1, protein (NM23A) expressed in
0.05	PDE1A	AW614381	phosphodiesterase 1A, calmodulin-dependent
0.05	NME7	AI094580	non-metastatic cells 7, protein expressed in (nucleoside-diphosphate kinase)
0.05	GUCY1B3	W93728	guanylate cyclase 1, soluble, beta 3
0.04	PRPS2	NM_002765	phosphoribosyl pyrophosphate synthetase 2
0.04	HPRT1	NM_000194	hypoxanthine phosphoribosyltransferase 1

Figure 2. Continued.

death observed in AD and PD, and Fas-induced cell apoptosis observed in AD, which have also been described in BSE (28).

Aside from numerous genes downregulated in this gCJD case, there are several genes showing upregulation. Among the 12 upregulated genes in sCJD described previously (6), eight genes were increased in G114V gCJD, including RAB13 (RAB13, member RAS oncogene family), inositol 1,4,5-trisphosphate 3-kinase B (ITPKB) and transcriptional coactivator with PDZ-binding motif (TAZ) that are more than 2-fold increased, and GFAP, cysteine and glycine-rich protein 1 (CSRP1), tropomyosin 2 (TPM2), promoting factor 1 (PTN) and RNA binding motif, single stranded interacting protein 3 (RBMS3) that are more than 1.5-fold increased. The proteins of the Rab family regulate specific tethering/docking of incoming vesicles to the correct target organelle (29), and they are involved in various biological processes, protein transport, small GTPase mediated signal transduction, vesicle-mediated transport, modification-dependent protein catabolism, ER to Golgi vesicle-mediated transport, endocytosis and some related regulation processes (12). Several Rab family members have been found to be associated with the PrP^{Sc} propagation and accumulation in the prion-infected cells (30), as well as with the clinical manifestations (31). In line with the observation in sCJD, Rab genes are unregulated in the cerebral cortex of G114V gCJD. These phenomena illustrate the similarity of gene expression profiles between G114V gCJD and sCJD. More up and downregulated genes in G114V gCJD rely heavily on the usage of a relatively larger capacity gene chip in this study. In addition, a series of genes that appeared dozens of times increased both in microarray and qRT-PCR will provide useful insights to further explore potential biomarkers for the diagnosis of CJD.

Acknowledgements

We thank Dr Christopher J. Vavricka from the Institute of Microbiology, Chinese Academy of Sciences, Beijing, China, for kindly checking the manuscript. This study was supported by the Chinese National Natural Science Foundation Grants 30800975, 81101302 and 30800640, the National Basic Research Program of China (973 Program) (2007CB310505), the China Mega-Project for Infectious Disease (2009ZX10004-101 and 2008ZX10004-008), and the SKLID Development Grant (2008SKLID102).

References

1. Prusiner SB: Prions. Proc Natl Acad Sci USA 95: 13363-13383, 1998.
2. Colby DW and Prusiner SB: Prions. Cold Spring Harb Perspect Biol 3: a006833, 2011.
3. Pastore M, Chin SS, Bell KL, *et al*: Creutzfeldt-Jakob disease (CJD) with a mutation at codon 148 of prion protein gene: relationship with sporadic CJD. Am J Pathol 167: 1729-1738, 2005.
4. Collins S, McLean CA and Masters CL: Gerstmann-Straussler-Scheinker syndrome, fatal familial insomnia, and kuru: a review of these less common human transmissible spongiform encephalopathies. J Clin Neurosci 8: 387-397, 2001.
5. Hwang D, Lee IY, Yoo H, *et al*: A systems approach to prion disease. Mol Syst Biol 5: 252, 2009.
6. Xiang W, Windl O, Westner IM, *et al*: Cerebral gene expression profiles in sporadic Creutzfeldt-Jakob disease. Ann Neurol 58: 242-257, 2005.
7. Ye J, Han J, Shi Q, *et al*: Human prion disease with a G114V mutation and epidemiological studies in a Chinese family: a case series. J Med Case Rep 2: 331, 2008.
8. Shi Q, Zhang BY, Gao C, *et al*: The diversities of PrP(Sc) distributions and pathologic changes in various brain regions from a Chinese patient with G114V genetic CJD. Neuropathology 32: 51-59, 2012.
9. Camon E, Magrane M, Barrell D, *et al*: The Gene Ontology Annotation (GOA) project: implementation of GO in SWISS-PROT, TrEMBL, and InterPro. Genome Res 13: 662-672, 2003.
10. NCBI GEO Profiles: National Center for Biotechnology Information, US National Library of Medicine, Bethesda, MD. http://www.ncbi.nlm.nih.gov/geo.
11. Mukherjee A and Soto C: Role of calcineurin in neurodegeneration produced by misfolded proteins and endoplasmic reticulum stress. Curr Opin Cell Biol 23: 223-230, 2011.
12. KEGG: Kyoto Encyclopedia of Genes and Genomes. http://www.genome.jp/kegg/.
13. Rodriguez MM, Peoc'h K, Haik S, *et al*: A novel mutation (G114V) in the prion protein gene in a family with inherited prion disease. Neurology 64: 1455-1457, 2005.
14. Kordek R, Liberski PP, Yanagihara R, Isaacson S and Gajdusek DC: Molecular analysis of prion protein (PrP) and glial fibrillary acidic protein (GFAP) transcripts in experimental Creutzfeldt-Jakob disease in mice. Acta Neurobiol Exp 57: 85-90, 1997.
15. Tang Y, Xiang W, Hawkins SA, Kretzschmar HA and Windl O: Transcriptional changes in the brains of cattle orally infected with the bovine spongiform encephalopathy agent precede detection of infectivity. J Virol 83: 9464-9473, 2009.
16. Martinez T and Pascual A: Identification of genes differentially expressed in SH-SY5Y neuroblastoma cells exposed to the prion peptide 106-126. Eur J Neurosci 26: 51-59, 2007.
17. Xiang W, Windl O, Wunsch G, *et al*: Identification of differentially expressed genes in scrapie-infected mouse brains by using global gene expression technology. J Virol 78: 11051-11060, 2004.
18. Zabel C, Nguyen HP, Hin SC, Hartl D, Mao L and Klose J: Proteasome and oxidative phoshorylation changes may explain why aging is a risk factor for neurodegenerative disorders. J Proteomics 73: 2230-2238, 2010.
19. Wikipedia website: http://en.wikipedia.org/wiki/Purine_metabolism.
20. Deriziotis P and Tabrizi SJ: Prions and the proteasome. Biochim Biophys Acta 1782: 713-722, 2008.
21. Li XL, Wang GR, Jing YY, *et al*: Cytosolic PrP induces apoptosis of cell by disrupting microtubule assembly. J Mol Neurosci 43: 316-325, 2011.
22. Nieznanski K, Podlubnaya ZA and Nieznanska H: Prion protein inhibits microtubule assembly by inducing tubulin oligomerization. Biochem Biophys Res Commun 349: 391-399, 2006.
23. Osiecka KM, Nieznanska H, Skowronek KJ, Karolczak J, Schneider G and Nieznanski K: Prion protein region 23-32 interacts with tubulin and inhibits microtubule assembly. Proteins 77: 279-296, 2009.
24. Fabrizi C, Silei V, Menegazzi M, *et al*: The stimulation of inducible nitric-oxide synthase by the prion protein fragment 106-126 in human microglia is tumor necrosis factor-alpha-dependent and involves p38 mitogen-activated protein kinase. J Biol Chem 276: 25692-25696, 2001.
25. Corsaro A, Thellung S, Villa V, *et al*: Prion protein fragment 106-126 induces a p38 MAP kinase-dependent apoptosis in SH-SY5Y neuroblastoma cells independently from the amyloid fibril formation. Ann NY Acad Sci 1010: 610-622, 2003.
26. Corsaro A, Thellung S, Chiovitti K, *et al*: Dual modulation of ERK1/2 and p38 MAP kinase activities induced by minocycline reverses the neurotoxic effects of the prion protein fragment 90-231. Neurotox Res 15: 138-154, 2009.
27. Higgins GC, Beart PM, Shin YS, Chen MJ, Cheung NS and Nagley P: Oxidative stress: emerging mitochondrial and cellular themes and variations in neuronal injury. J Alzheimers Dis 20 (Suppl 2): S453-S473, 2010.
28. Tang Y, Xiang W, Terry L, Kretzschmar HA and Windl O: Transcriptional analysis implicates endoplasmic reticulum stress in bovine spongiform encephalopathy. PLoS One 5: e14207, 2010.
29. Zerial M and McBride H: Rab proteins as membrane organizers. Nat Rev Mol Cell Biol 2: 107-117, 2001.
30. Gilch S, Bach C, Lutzny G, Vorberg I and Schatzl HM: Inhibition of cholesterol recycling impairs cellular PrP(Sc) propagation. Cell Mol Life Sci 66: 3979-3991, 2009.
31. Ermolayev V, Cathomen T, Merk J, *et al*: Impaired axonal transport in motor neurons correlates with clinical prion disease. PLoS Pathog 5: e1000558, 2009.